

# Perspectives on Additive Manufacturing Enabled Beta-Titanium Alloys for Biomedical Applications

Swee Leong Sing<sup>1,2\*</sup>

<sup>1</sup>Department of Mechanical Engineering, National University of Singapore, Singapore

<sup>2</sup>Singapore Centre for 3D Printing, School of Mechanical and Aerospace Engineering, Nanyang Technological University, Singapore

**Abstract:** “Stress shielding” caused by the mismatch of modulus between the implant and natural bones, is one of the major problems faced by current commercially used biomedical materials. Beta-titanium ( $\beta$ -Ti) alloys are a class of materials that have received increased interest in the biomedical field due to their relatively low elastic modulus and excellent biocompatibility. Due to their lower modulus,  $\beta$ -Ti alloys have the potential to reduce “stress shielding.” Powder bed fusion (PBF), a category of additive manufacturing, or more commonly known as 3D printing techniques, has been used to process  $\beta$ -Ti alloys. In this perspective article, the emerging research of PBF of  $\beta$ -Ti alloys is covered. The potential and limitations of using PBF for these materials in biomedical applications are also elucidated with focus on the perspectives from processes, materials, and designs. Finally, future trends and potential research topics are highlighted.

**Keywords:** Additive manufacturing; 3D printing; Powder bed fusion; Selective laser melting; Electron beam melting; Titanium

\*Correspondence to: Swee Leong Sing, Department of Mechanical Engineering, National University of Singapore, Singapore; [sweeleong.sing@nus.edu.sg](mailto:sweeleong.sing@nus.edu.sg)

**Received:** December 3, 2021; **Accepted:** December 21, 2021; **Published Online:** January 12, 2022

(This article belongs to the *Special Section: 3D Printing and Bioprinting for the Future of Healthcare*)

**Citation:** Sing S L. 2022, Perspectives on Additive Manufacturing Enabled Beta-Titanium Alloys for Biomedical Applications. *Int J Bioprint*, 8(1):478. <http://doi.org/10.18063/ijb.v8i1.478>

## 1. Introduction

Powder bed fusion (PBF) is a group of additive manufacturing (AM) or three-dimensional (3D) printing techniques. When equipped with lasers as energy sources, the processes are also known as laser powder bed fusion (L-PBF). L-PBF is also commercially known as selective laser melting (SLM) or direct metal laser melting<sup>[1,2]</sup>. Another type of PBF process uses electron beam as the energy source and thus is known as electron beam powder bed fusion (EB-PBF) or commercially as selective electron beam melting. These manufacturing processes have shown successes in processing alloys<sup>[3]</sup> and even ceramics<sup>[4,5]</sup>. Like any other AM techniques, PBF has the capability to fabricate functional parts with complex geometry due to its freeform fabrication capabilities. The process starts from designing of the parts using a computer-aided design (CAD) software and exporting the data files into the PBF equipment. The data files are also

first input with process parameters and then sliced into two-dimensional cross sections. The PBF process itself involves a cycle of depositing powder layers onto the build platform or previously processed layers, then the melting of the powder selectively using laser or electron beam. The areas that are melted follow the cross sections from the sliced CAD data file. After this step, the build platform is then lowered and a new powder layer is deposited. The cycle repeats until the full 3D components are fabricated<sup>[6]</sup>. As a result of the cyclic process and repeated thermal cycles, the materials undergo solid-liquid-solid phase transformations<sup>[7]</sup>. These unique physical phenomena bring about the microstructural changes which affect the mechanical properties of the materials. The detailed PBF process is also described elsewhere<sup>[8-11]</sup>. A schematic of the PBF process is shown in **Figure 1**.

Most of the current materials used for biomedical implants commercially, such as 316L stainless steel, CoCrMo, and even Ti6Al4V, have a problem which is the

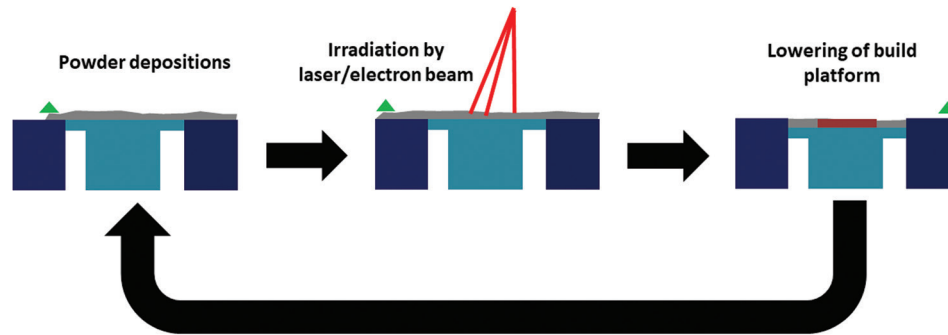


**Figure 1.** Powder bed fusion process.

mismatch of their modulus to that of natural bones. While the elastic modulus of human cortical bone ranges from 17.6 to 28 GPa, that of CoCrMo and 316L stainless steel is more than 200 GPa<sup>[12]</sup> and even Ti6Al4V has elastic modulus of approximate 130 GPa<sup>[13]</sup>. These are many times higher than that of human cortical bone even when they are commonly used<sup>[14]</sup>. Osteolysis can be attributed to this modulus mismatch as it lessens the loading on the natural bones that are neighboring the implant, leading to bone resorption. Finally, implant loosening would occur.

Recently, due to their higher strength, lower modulus and better corrosion resistance, beta-titanium ( $\beta$ -Ti) alloys have been identified as potential materials to improve implants quality<sup>[7,15,16]</sup>.  $\beta$ -Ti alloys are titanium alloys where the  $\beta$ -phase is significantly retained in equilibrium or at least on quenching from the  $\beta$ -phase without transformation into martensite or  $\alpha$ -phase<sup>[7]</sup>. Furthermore,  $\beta$ -Ti alloys usually consist of non-toxic elements such as tantalum, niobium, molybdenum, tin, and zirconium. To obtain  $\beta$ -Ti alloys that are biocompatible, niobium and tantalum which are  $\beta$ -phase stabilizers for titanium are the common choices for alloying elements due to their high biocompatibility. The other elements such as zirconium, molybdenum, and tin are added to further modify phases and microstructures of the  $\beta$ -Ti alloys.

In this article, an overview of the processing, microstructure, and properties of  $\beta$ -Ti alloys processed by PBF that can be used in biomedical applications is discussed. The potential and limitations of using PBF for these materials in biomedical applications are also elucidated with focus on the perspectives from processes, materials, and designs. Finally, future trends and potential research topics are highlighted.

## 2. $\beta$ -Titanium alloys by powder bed fusion

### 2.1. Powder bed fusion

It is important to understand the physical phenomena that occur during the PBF process to obtain parts with good quality, that is, parts that are defect free. For functional applications of PBF parts, defects can have detrimental

effects on wear and corrosion resistance which have to be avoided for biomedical applications. The complex PBF process involves multitude of physical phenomena, such as thermal energy absorption, reflection, and transfers. Phase transformations such as solid to liquid and then back to solid also occur<sup>[17,18]</sup>.

For low modulus  $\beta$ -Ti alloys that are often metastable, a high cooling rate during the manufacturing process is required to retain the  $\beta$ -phase<sup>[19]</sup>. As such, PBF is inherently designed for this due to the rapid solidification and cooling cycles that occur in the process<sup>[20]</sup>. However, many defects such as porosity, balling, oxide inclusions, and cracking remain as metallurgical challenges for PBF. The details of these defects and their forming mechanisms have been discussed in recent reviews<sup>[21,22]</sup>. To minimize these defects in PBF parts, the effect of process parameters on the parts quality has been studied extensively. The commonly investigated L-PBF process parameters include laser power ( $P$ ), scanning speed ( $v$ ), hatch spacing ( $h$ ), and layer thickness ( $d$ ) and they are often discussed using one equation:

$$\varepsilon = \frac{P}{v \cdot h \cdot d} \quad (1)$$

where,  $\varepsilon$  is termed as the volumetric energy density<sup>[23,24]</sup>.

For EB-PBF, the key process parameters include acceleration voltage ( $V$ ), beam current ( $I$ ), scanning speed ( $v$ ), hatch spacing ( $h$ ), and layer thickness ( $d$ ). They are also often discussed using one equation:

$$\varepsilon = \frac{VI}{v \cdot h \cdot d} \quad (2)$$

where,  $\varepsilon$  is also the volumetric energy density<sup>[25,26]</sup>. Equation (ii) can be expressed as Equation (i) in which  $P = VI$  where  $P$  is the beam power<sup>[27,28]</sup>.

As an example to elucidate the process parameters effect on  $\beta$ -Ti alloys, the fabrication of Ti53Nb using

volumetric energy densities from 16 to 317 J/mm<sup>3</sup> was investigated<sup>[24]</sup>. The porosity present in the samples is formed due to incomplete fusion and overmelting. As observed for laser power of 100 W and 200 W, increasing scanning speed led to increasing lack of fusion pores<sup>[24]</sup>. It is common to have pores formation as a result of trapped gas or vapor during overmelting. In another study done, also using Ti53Nb (wt%), volumetric energy density between 32 and 95 J/mm<sup>3</sup> was used, relative density of the samples ranged from 87% to above 99%<sup>[29]</sup>. Due to the high niobium content, the samples maintained the  $\beta$ -phase with no phase transformation<sup>[30]</sup>.

## 2.2. Properties of $\beta$ -titanium alloys

Research on AM of  $\beta$ -Ti alloys confirmed the appearance of complex martensitic phases, the transformation of martensitic phases, and the improvement of mechanical properties<sup>[31]</sup>. In a study on Ti45Nb (wt%), X-ray diffraction patterns on the L-PBF part show  $\beta$ -Ti peaks with broadening characteristics possibly due to residual stresses in the parts<sup>[32]</sup>. The samples showed a compressive strength of 723 MPa. Another study was also done on Ti42Nb (wt%)<sup>[33]</sup>. In the work done on Ti53Nb (wt%), metastable  $\beta$ -phase is also reported<sup>[29]</sup>. A study done using Ti15Mo3Nb3Al0.2Si (wt%) showed the as-built parts exhibited columnar grains of  $\beta$ -phase oriented along the build direction. The samples also have microhardness of 278 HV, yield strength of 917 MPa, ultimate tensile strength of 946 MPa with ductility of 25.3%<sup>[34]</sup>. A study done on Ti52Nb (wt%) shows that the scanning speed and laser power, or potentially any process parameters, have effect on the elastic modulus of the material. One of the parameters set obtained Young's modulus of  $70.5 \pm 1.5$  GPa<sup>[30]</sup>. Schwab *et al.* studied the fabrication of Ti5Al5V5Mo3Mo (wt%) using L-PBF and were able to achieve relative density of 99.5%. The samples also showed an ultimate tensile strength of 800 MPa and maximum elongation of 14%<sup>[35]</sup>. In another study using Ti25Nb3Zr3Mo2Sn, the samples have ultimate tensile strength of  $716 \pm 14$  MPa and ductility of  $37 \pm 5\%$ <sup>[36]</sup>. Using Ti24Nb4Zr8Sn, L-PBF samples have Young's modulus of  $53 \pm 1$  GPa, ultimate tensile strength of  $665 \pm 18$  MPa, yield strength of  $563 \pm 38$  MPa, and elongation of  $13.8 \pm 4.1\%$ <sup>[37]</sup>. In a study using Ti35Nb7Zr5Ta (wt%), relative density of more than 99.8% was obtained. The alloy exhibits an ultimate tensile strength of 631 MPa while having a low modulus of approximately 81 GPa<sup>[16]</sup>. The same alloy was also fabricated using EB-PBF and has a modulus of 92 GPa<sup>[38]</sup>. Wang *et al.* studied the fabrication of Ti24Nb4Zr8Sn using EB-PBF, however, no mechanical characterizations were conducted<sup>[39]</sup>. Sun *et al.* studied the fabrication of Ti15Mo5Zr3Al using both L-PBF and EB-PBF. It is shown that the L-PBF samples have higher ductility but lower strength when compared to the EB-PBF samples<sup>[28]</sup>.

## 3. Potential research for $\beta$ -titanium alloys by PBF

### 3.1. In situ alloying

*In situ* alloying using PBF, especially L-PBF, which uses powder mixtures instead of the typical pre-alloyed powders, has been popular to achieve  $\beta$ -Ti alloys. The past studies showed that this approach can be used to obtain  $\beta$ -Ti alloys with desirable properties<sup>[40,41]</sup>. For example, Wang *et al.* used *in situ* alloying with L-PBF and found that the niobium addition into titanium leads to better *in vitro* apatite forming capability as compared to pure titanium<sup>[42]</sup>. In a similar study done using *in situ* alloying of Ti25Nb (wt%), better cell spread and proliferation are observed when the alloy is benchmarked with titanium. The  $\beta$ -Ti alloy also has superior *in vitro* appetite forming capability<sup>[43]</sup>. Using EB-PBF, *in situ* alloying of Ti10Nb (at%) was done. It was concluded that  $\beta$ -phase is dominant in the resulting alloy<sup>[44]</sup>. Comprehensive reviews on *in situ* alloying have been conducted previously<sup>[21,45]</sup>. Comparison between typical PBF and *in situ* alloying is shown in Figure 2.

### 3.2. Designed porosity for $\beta$ -titanium alloys

There is a limitation to the minimum elastic modulus that can be achieved just by developing new materials. As such, an alternative solution to achieve modulus matching between the implants and bone is by introducing designed and controlled porosity to the materials. Porous lattice structures can be fabricated by L-PBF due to its capability for freeform fabrication<sup>[46-48]</sup>. Coupling these structures with suitable alloys such as the  $\beta$ -Ti alloys, AM can potentially produce biomedical implants that meet the stiffness and strength criteria while achieving excellent osseointegration. In their work, Hafeez *et al.* fabricated porous structures with different pore dimensions using Ti35Nb2Ta3Zr by L-PBF. They maintained the porosity for these structures at around 50% and are able to obtain modulus of approximately 3.1 GPa, which is quite close to the modulus of bones<sup>[49]</sup>. Porous lattice structures were

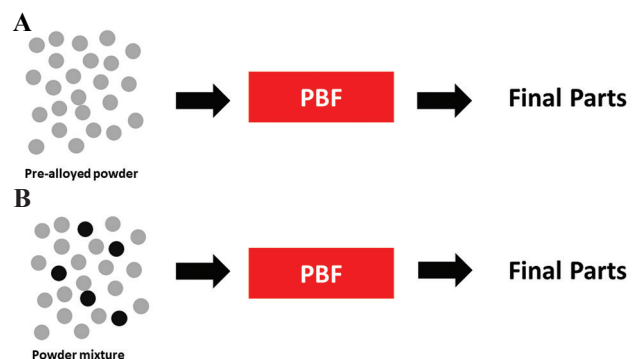


**Figure 2.** Powder bed fusion process. (A) Typical approach. (B) In situ alloying.

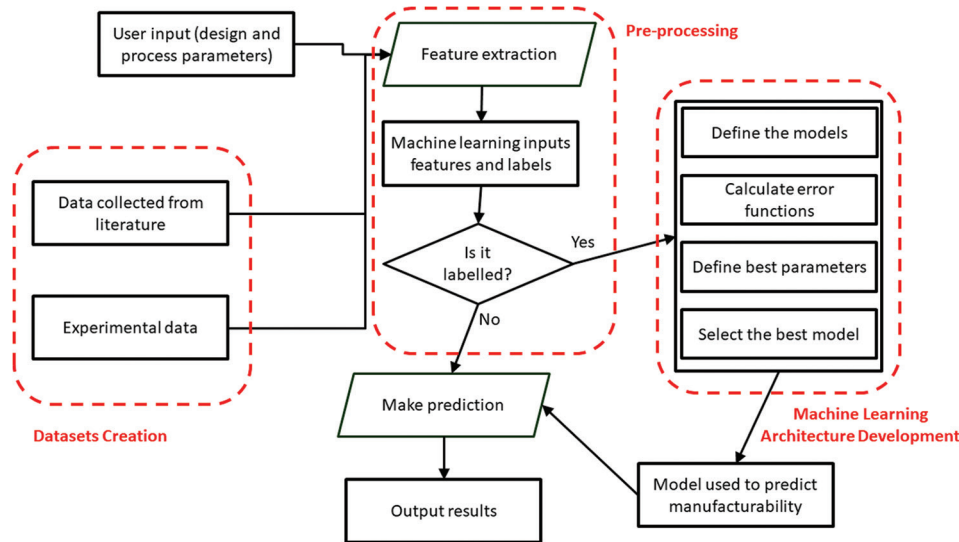


**Figure 3.** A conceptual framework for predicting manufacturability for powder bed fusion using machine learning.

also fabricated using Ti24Nb4Zr8Sn and the samples have Young's modulus of  $0.95 \pm 0.05$  GPa<sup>[50]</sup>. Porous lattice structures are also fabricated using  $\beta$ -phase Ti24Nb4Zr8Sn<sup>[51]</sup>. Ti35Zr28Nb was used to fabricate porous lattice structures with FCCZ and FBCCZ unit cells. While the bulk material elastic modulus is between  $57.0 \pm 1.8\%$  GPa, the porous lattice structures are able to achieve elastic modulus of between  $1.1 \pm 0.1\%$  GPa and  $1.3 \pm 0.1\%$  GPa<sup>[52]</sup>. It was also concluded that the structures have good corrosion behavior and biocompatibility. Using Ti25Nb3Zr3Mo2Sn to fabricate porous lattice structures by L-PBF, Liu *et al.* found out that martensitic phase transformation takes place during yielding under compression loading for the samples, which prevents the samples from layer-wise fracture<sup>[53]</sup>. Such phase transformation is also found to improve the tensile strength of  $\beta$ -Ti alloys<sup>[54]</sup>. Using EB-PBF, Liu *et al.* fabricated porous structures made of Ti24Nb4Zr8Sn and compared the effect of different designed porosities<sup>[55]</sup>.

### 3.3. Machine learning and artificial intelligence

The fluctuations in L-PBF make process control and prediction challenging. While physical simulations have been developed to provide deeper understanding of the process, it is still challenging for them to show the full aspects of L-PBF. Machine learning and artificial intelligence can be used to enhance and complement simulations in achieving higher part quality<sup>[56]</sup>. The current practice to obtain defect-free parts, or commonly known as the process parameters optimization, involves multiple rounds of experiments which are costly and time intensive. Machine learning techniques potentially can be applied to establish relationships between

the input and output of L-PBF. Smaller data sets can be used to develop and train the machine learning algorithms by measuring the part quality from different process parameters. Predictive models using genetic programming and neural network modeling for process planning purposes have been developed for L-PBF<sup>[57]</sup>. Deep neural networks can also be used to interpret and classify melt pool images that can be used to predict the defects during the process<sup>[58,59]</sup>. Shin *et al.* developed an artificial neural network to identify the optimum L-PBF process parameters to obtain defect-free Ti5Al5V5Mo3Cr (wt%) and showed the potential of using this approach to reduce processing time and making the L-PBF process more cost effective<sup>[60]</sup>. A conceptual framework on using machine learning to predict manufacturability for PBF is shown in **Figure 3**.

Comprehensive reviews on machine learning for AM are available<sup>[56,61-63]</sup>. Using data-driven artificial intelligence, it is possible to predict and optimize process parameters that can obtain desired part properties<sup>[64,65]</sup>. Furthermore, a conceptual framework that combines statistical analysis, mathematical modeling, and machine learning techniques has also been proposed<sup>[66]</sup>.

## 4. Summary

In this perspective article, the feasibility of processing  $\beta$ -Ti alloys using PBF has been shown using currently available literature. It has been shown that these alloys have potential to be better candidates for biomedical implants due to their lower elastic modulus and high mechanical strength. However, to realize their full potential, future research in the area of new processing approaches and new designs are still needed.



## Acknowledgments

The author acknowledges the support from NTU Presidential Postdoctoral Fellowship from Nanyang Technological University, Singapore.

## Conflict of interest

The author declared no known conflict of interest.

## References

- Liu ZH, Zhang DQ, Chua CK, *et al.*, 2013. Crystal Structure Analysis of M2 High Speed Steel Parts Produced by Selective Laser Melting. *Mater Characterization*, 84:72–80. <https://doi.org/10.1016/j.matchar.2013.07.010>
- Sing SL, Yeong WY, Wiria FE, *et al.*, 2016. Characterization of Titanium Lattice Structures Fabricated by Selective Laser Melting Using an Adapted Compressive Test Method. *Exp Mech*, 56:735–48. <https://doi.org/10.1007/s11340-015-0117-y>
- Herzog D, Seyda V, Wycisk E, *et al.*, 2016. Additive Manufacturing of Metals. *Acta Mater*, 117:371–92. <https://doi.org/10.1016/j.actamat.2016.07.019>
- Sing SL, Yeong WY, Wiria FE, *et al.*, 2017. Direct Selective Laser Sintering and Melting of Ceramics: A Review. *Rapid Prototyp J*, 23:611–23. <https://doi.org/10.1108/rpj-11-2015-0178>
- Yap CY, Chua CK, Dong ZL, *et al.*, 2015. Review of Selective Laser Melting: Materials and Applications. *Appl Phys Rev*, 2:041101. <https://doi.org/10.1063/1.4935926>
- Bogue R, 2011. Nanocomposites: A Review of Technology and Applications. *Assembly Autom*, 31:106–12.
- Colombo-Pulgarin JC, Biffi CA, Vedani M, *et al.*, 2021. Beta Titanium Alloys Processed By Laser Powder Bed Fusion: A Review. *J Mater Eng Perform*, 30:6365–88. <https://doi.org/10.1007/s11665-021-05800-6>
- DebRoy T, Wei HL, Zuback JS, *et al.*, 2018. Additive Manufacturing of Metallic Components Process, Structure and Properties. *Prog Mater Sci*, 92:112–224. <https://doi.org/10.1016/j.pmatsci.2017.10.001>
- Gu DD, Meiners W, Wissenbach K, *et al.*, 2013. Laser Additive Manufacturing of Metallic Components: Materials, Processes and Mechanisms. *Int Mater Rev*, 57:133–64. <https://doi.org/10.1179/1743280411y.0000000014>
- Olakanmi EO, Cochrane RF, Dalgarno KW, 2015. A Review on Selective Laser Sintering/Melting (SLS/SLM) of Aluminium Alloy Powders: Processing, Microstructure, and Properties. *Prog Mater Sci*, 74:401–77. <https://doi.org/10.1016/j.pmatsci.2015.03.002>
- Sercombe TB, Li X, 2016. Selective laser melting of aluminium and aluminium metal matrix composites: A review. *Mater Technol* 2016;31:77-85. <https://doi.org/10.1179/1753555715y.0000000078>
- Li Y, Yang C, Zhao H, *et al.*, 2014. New Developments of Ti-based Alloys for Biomedical Applications. *Materials*, 7:1709–800. <https://doi.org/10.3390/ma7031709>
- Niinomi M. Recent Metallic Materials for Biomedical Applications. *Metallurgical Mater Trans A*, 2002;33:477. <https://doi.org/10.1007/s11661-002-0109-2>
- Yang CL, Zhang ZJ, Li SJ, *et al.*, 2018. Simultaneous Improvement in Strength and Plasticity of Ti-24Nb-4Zr-8Sn Manufactured by Selective Laser Melting. *Mater Des*, 157:52–9. <https://doi.org/10.1016/j.matdes.2018.07.036>
- Kuroda D, Niinomi M, Morinaga M, *et al.*, 1998. Design and Mechanical Properties of New  $\beta$  Type Titanium Alloys for Implant Materials. *Mater Sci Eng A*, 243:244–9. [https://doi.org/10.1016/S0921-5093\(97\)00808-3](https://doi.org/10.1016/S0921-5093(97)00808-3)
- Ummethala R, Karamched PS, Rathinavelu S, *et al.*, 2020. Selective Laser Melting of High-strength, Low-modulus Ti-35Nb-7Zr-5Ta alloy. *Materialia*, 14:100941. <https://doi.org/10.1016/j.mtla.2020.100941>
- Yadroitsev I, Gusarov AV, Yadroitsava I, *et al.*, 2010. Single Track Formation in Selective Laser Melting of Metal Powders. *J Mater Proc Technol*, 210:1624–31. <https://doi.org/10.1016/j.jmatprotec.2010.05.010>
- Markl M, Körner C, 2016, Multiscale Modeling of Powder Bed-Based Additive Manufacturing. *Ann Rev Mater Res*, 46:93–123. <https://doi.org/10.1146/annurev-matsci-070115-032158>
- Aleixo GT, Afonso C, Coelho A, *et al.*, 2008. Effects of Omega Phase on Elastic Modulus of Ti-Nb Alloys as a Function of Composition and Cooling Rate. *Solid State Phenomena*, 138:393–8. <https://doi.org/10.4028/www.scientific.net/SSP.138.393>
- Mantri SA, Nartu MS, Dasari S, *et al.*, 2021. Suppression and Reactivation of Transformation and Twinning Induced Plasticity in Laser Powder Bed Fusion Additively Manufactured Ti-10V-2Fe-3Al. *Addit Manuf*, 48:102406.
- Sing SL, Huang S, Goh GD, *et al.*, 2021. Emerging Metallic Systems for Additive Manufacturing: *In-Situ* Alloying and Multi-metal Processing in Laser Powder Bed Fusion. *Prog Mater Sci*, 119:100795.

- <https://doi.org/10.1016/j.pmatsci.2021.100795>
22. Yu WH, Sing SL, Chua CK, *et al.*, 2019. Particle-Reinforced Metal Matrix Nanocomposites Fabricated by Selective Laser Melting: A State of the Art Review. *Prog Mater Sci*, 104:330–79. <https://doi.org/10.1016/j.pmatsci.2019.04.006>
  23. Saedi S, Moghaddam NS, Amerinatanzi A, *et al.*, 2018. On the Effects of Selective Laser Melting Process Parameters on Microstructure and Thermomechanical Response of Ni-rich NiTi. *Acta Mater*, 144:552–60. <https://doi.org/10.1016/j.actamat.2017.10.072>
  24. Guzmán J, de Moura Nobre R, Nunes ER, *et al.*, 2021. Laser Powder Bed Fusion Parameters to Produce High-density Ti-53%Nb Alloy Using Irregularly Shaped Powder from Hydride-dehydride (HDH) Process. *J Mater Res Technol*, 10:1372–81. <https://doi.org/10.1016/j.jmrt.2020.12.084>
  25. Silvestri AT, Foglia S, Borrelli R, *et al.*, 2020. Electron Beam Melting of Ti6Al4V: Role of the Process Parameters under the Same Energy Density. *J Manuf Processes*, 60:162–79. <https://doi.org/10.1016/j.jmapro.2020.10.065>
  26. Pobel CR, Osmanlic F, Lodes MA, *et al.*, 2019. Processing Windows for Ti-6Al-4V Fabricated by Selective Electron Beam Melting with Improved Beam Focus and Different Scan Line Spacings. *Rapid Prototyp J*, 25:665–71. <https://doi.org/10.1108/RPJ-04-2018-0084>
  27. Sabzi HE, 2019. Powder Bed Fusion Additive Layer Manufacturing of Titanium Alloys. *Mater Sci Technol*, 35:875–90. <https://doi.org/10.1080/02670836.2019.1602974>
  28. Sun SH, Hagihara K, Ishimoto T, *et al.*, 2021. Comparison of Microstructure, Crystallographic Texture, and Mechanical Properties in Ti-15Mo-5Zr-3Al Alloys Fabricated Via Electron and Laser Beam Powder Bed Fusion Technologies. *Addit Manuf*, 47:102329. <https://doi.org/10.1016/j.addma.2021.102329>
  29. Guzmán J, de Moura Nobre R, Rodrigues Júnior DL, *et al.*, 2021. Comparing Spherical and Irregularly Shaped Powders in Laser Powder Bed Fusion of Nb47Ti Alloy. *J Mater Eng Perf*, 30:6557–67. <https://doi.org/10.1007/s11665-021-05916-9>
  30. De Moura Nobre R, Ank de Morais W, Vasques MT, *et al.*, 2021. Role of Laser Powder Bed Fusion Process Parameters in Crystallographic Texture of Additive Manufactured Nb-48Ti Alloy. *J Mater Res Technol*, 14:484–95. <https://doi.org/10.1016/j.jmrt.2021.06.054>
  31. Hafeez N, Wei D, Xie L, *et al.*, 2021. Evolution of Microstructural Complex Transitions in Low-modulus  $\beta$ -type Ti-35Nb-2Ta-3Zr Alloy Manufactured by Laser Powder Bed Fusion. *Addit Manuf*, 48:102376. <https://doi.org/10.1016/j.addma.2021.102376>
  32. Schwab H, Prashanth K, Löber L, *et al.*, 2015. Selective Laser Melting of Ti-45Nb Alloy. *Metals*, 5:686–94. <https://doi.org/10.3390/met5020686>
  33. Schulze C, Weinmann M, Schweigel C, *et al.*, 2018. Mechanical Properties of a Newly Additive Manufactured Implant Material Based on Ti-42Nb. *Materials*, 11:124. <https://doi.org/10.3390/ma11010124>
  34. Macias-Sifuentes MA, Xu C, Sanchez-Mata O, *et al.*, 2021. Microstructure and Mechanical Properties of  $\beta$ -21S Ti Alloy Fabricated through Laser Powder Bed Fusion. *Prog Addit Manuf*, 6:417–30. <https://doi.org/10.1007/s40964-021-00181-7>
  35. Schwab H, Palm F, Kuhn U, *et al.*, 2016. Microstructure and Mechanical Properties of the Near-beta Titanium Alloy Ti-5553 Processed by Selective Laser Melting. *Mater Des*, 105:75–80. <https://doi.org/10.1016/j.matdes.2016.04.103>
  36. Liu YJ, Zhang YS, Zhang LC, 2019. Transformation-induced Plasticity and High Strength in Beta Titanium Alloy Manufactured by Selective Laser Melting. *Materialia*, 6:100299. <https://doi.org/10.1016/j.mtla.2019.100299>
  37. Zhang LC, Klemm D, Eckert J, *et al.*, 2011. Manufacture by Selective Laser Melting and Mechanical Behavior of a Biomedical Ti-24Nb-4Zr-8Sn Alloy. *Scripta Mater*, 65:21–4. <https://doi.org/10.1016/j.scriptamat.2011.03.024>
  38. Surmeneva M, Grubova I, Glukhova N, *et al.*, 2021. New Ti-35Nb-7Zr-5Ta Alloy Manufacturing by Electron Beam Melting for Medical Application Followed by High Current Pulsed Electron Beam Treatment. *Metals*, 11:1066. <https://doi.org/10.3390/met11071066>
  39. Wang Q, Zhang W, Li S, *et al.*, 2021. Material Characterisation and Computational Thermal Modelling of Electron Beam Powder Bed Fusion Additive Manufacturing of Ti2448 Titanium Alloy. *Materials*, 14:7359. <https://doi.org/10.3390/ma14237359>
  40. Poozov I, Sufiarov V, Popovich A, *et al.*, 2018. Synthesis of Ti-5Al, Ti-6Al-7Nb, and Ti-22Al-25Nb Alloys from Elemental Powders Using Powder-bed Fusion Additive Manufacturing. *J Alloys Comp*, 763:436–45. <https://doi.org/10.1016/j.jallcom.2018.05.325>
  41. Kang N, Lu Y, Lin X, *et al.*, 2019. Microstructure and Tensile Properties of Ti-Mo Alloys Manufactured via Using Laser Powder Bed Fusion. *J Alloys Comp*, 771:877–84. <https://doi.org/10.3390/cryst11091064>

42. Wang Q, Han C, Choma T, *et al.*, 2017. Effect of Nb Content on Microstructure, Property and *In Vitro* Apatite-forming Capability of Ti-Nb Alloys Fabricated via Selective Laser Melting. *Mater Des*, 126:268–77.  
<https://doi.org/10.1016/j.matdes.2017.04.026>
43. Zhao D, Han C, Li J, *et al.*, 2020. *In Situ* Fabrication of a Titanium-niobium Alloy with Tailored Microstructures, Enhanced Mechanical Properties and Biocompatibility by Using Selective Laser Melting. *Mater Sci Eng C*, 2020:110784.  
<https://doi.org/10.1016/j.msec.2020.110784>
44. Surmeneva MA, Koptuyg A, Khrapov D, *et al.*, 2020. *In Situ* Synthesis of a Binary Ti-10at% Nb Alloy by Electron Beam Melting Using a Mixture of Elemental Niobium and Titanium Powders. *J Mater Proc Technol*, 282:116646.  
<https://doi.org/10.1016/j.jmatprotec.2020.116646>
45. Mosallanejad MH, Niroumand B, Aversa A, *et al.*, 2021. *In-Situ* Alloying in Laser-based Additive Manufacturing Processes: A Critical Review. *J Alloys Comp*, 872:159567.  
<https://doi.org/10.1016/j.jallcom.2021.159567>
46. Sing SL, Wiria FE, Yeong WY, 2018. Selective Laser Melting of Lattice Structures: A Statistical Approach to Manufacturability and Mechanical Behavior. *Robot Comput Integr Manuf*, 49:170–80.  
<https://doi.org/10.1016/j.rcim.2017.06.006>
47. Sing SL, Wiria FE, Yeong WY, 2018. Selective Laser Melting of Titanium Alloy with 50 wt% Tantalum: Effect of Laser Process Parameters on Part Quality. *Int J Refract Metals Hard Mater*, 77:120–7.  
<https://doi.org/10.1016/j.ijrmhm.2018.08.006>
48. Yang Y, Wang G, Liang H, *et al.*, 2019. Additive Manufacturing of Bone Scaffolds. *Int J Bioprint*, 5:148.  
<https://doi.org/10.18063/IJB.v5i1.148>
49. Hafeez N, Liu J, Wang L, *et al.*, 2020. Superelastic Response of Low-modulus Porous Beta-type Ti-35Nb-2Ta-3Zr Alloy Fabricated by Laser Powder Bed Fusion. *Addit Manuf*, 34:101264.  
<https://doi.org/10.1016/j.addma.2020.101264>
50. Liu YJ, Li SJ, Wang HL, *et al.*, 2016. Microstructure, Defects and Mechanical Behavior of Beta-type Titanium Porous Structures Manufactured by Electron Beam Melting and Selective Laser Melting. *Acta Mater*, 113:56–67.  
<https://doi.org/10.1016/j.actamat.2016.04.029>
51. Liu YJ, Li SJ, Zhang LC, *et al.*, 2018. Early Plastic Deformation Behaviour and Energy Absorption in Porous  $\beta$ -type Biomedical Titanium Produced by Selective Laser Melting. *Script Mater*, 153:99–103.  
<https://doi.org/10.1016/j.scriptamat.2018.05.010>
52. Li Y, Ding Y, Munir K, *et al.*, 2019. Novel  $\beta$ -Ti35Zr28Nb Alloy Scaffolds Manufactured Using Selective Laser Melting for Bone Implant Applications. *Acta Biomater*, 87:273–84.  
<https://doi.org/10.1016/j.actbio.2019.01.051>
53. Liu YJ, Zhang JS, Liu XC, *et al.*, 2021. Non-layer-wise Fracture and Deformation Mechanism in Beta Titanium Cubic Lattice Structure Manufactured by Selective Laser Melting. *Mater Sci Eng A*, 822:141696.  
<https://doi.org/10.1016/j.msea.2021.141696>
54. Qiu C, Liu Q, Ding R, 2021. Significant Enhancement in Yield Strength for a Metastable Beta Titanium Alloy by Selective Laser Melting. *Mater Sci Eng A*, 816:141291.  
<https://doi.org/10.1016/j.msea.2021.141291>
55. Liu YJ, Wang HL, Li SJ, *et al.*, 2017. Compressive and Fatigue Behavior of Beta-type Titanium Porous Structures Fabricated by Electron Beam Melting. *Acta Mater*, 126:58–66.  
<https://doi.org/10.1016/j.actamat.2016.12.052>
56. Goh GD, Sing SL, Yeong WY, 2020. A Review on Machine Learning in 3D Printing: Applications, Potential, and Challenges. *Artif Intell Rev*, 54:63–94.  
<https://doi.org/10.1007/s10462-020-09876-9>
57. Özel T, Altay A, Kaftanoğlu B, *et al.*, 2020. Focus Variation Measurement and Prediction of Surface Texture Parameters Using Machine Learning in Laser Powder Bed Fusion. *J Manuf Sci Eng*, 12:011008.  
<https://doi.org/10.1115/1.4045415>
58. Kwon O, Kim HG, Ham MJ, *et al.*, 2020. A Deep Neural Network for Classification of Melt-pool Images in Metal Additive Manufacturing. *J Intell Manuf*, 31:375–86.  
<https://doi.org/10.1007/s10845-018-1451-6>
59. Kunkel MH, Gebhardt A, Mpofo K, *et al.*, 2019. Quality Assurance in Metal Powder Bed Fusion Via Deep-learning-Based Image Classification. *Rapid Prototyp J*, 26:259–66.  
<https://doi.org/10.1108/RPJ-03-2019-0066>
60. Shin DS, Lee CH, Kuhn U, *et al.*, 2021. Optimizing Laser Powder Bed Fusion of Ti-5Al-5V-5Mo-3Cr by Artificial Intelligence. *J Alloys Comp*, 862:158018.  
<https://doi.org/10.1016/j.jallcom.2020.158018>
61. Meng L, McWilliams B, Jarosinski W, *et al.*, 2020. Machine Learning in Additive Manufacturing: A Review. *JOM*, 72:2363–77.  
<https://doi.org/10.1007/s11837-020-04155-y>
62. Qi X, Chen G, Li Y, *et al.*, 2019. Applying Neural-Network-Based Machine Learning to Additive Manufacturing: Current Applications, Challenges, and Future Perspectives. *Engineering*. 5:721–9.

- <https://doi.org/10.1016/j.eng.2019.04.012>
63. Sing SL, Kuo CN, Shih CT, *et al.*, 2021. Perspectives of Using Machine Learning in Laser Powder Bed Fusion for Metal Additive Manufacturing. *Virtual Phys Prototyp*, 2021;16:372–86.  
<https://doi.org/10.1080/17452759.2021.1944229>
64. Rudolph JP, Emmelmann C, 2018. Self-learning Calculation for Selective Laser Melting. *Proc CIRP*, 67:185–90.  
<https://doi.org/10.1016/j.procir.2017.12.197>
65. Renken V, Albinger S, Goch G, *et al.*, 2017. Development of an Adaptive, Self-learning Control Concept for an Additive Manufacturing Process. *CIRP J Manuf Sci Technol*, 19:57–61.  
<https://doi.org/10.1016/j.cirpj.2017.05.002>
66. Baturynska I, Semeniuta O, Martinsen K, 2018. Optimization of Process Parameters for Powder Bed Fusion Additive Manufacturing by Combination of Machine Learning and Finite Element Method: A Conceptual Framework. *Proc CIRP*, 67:227–32.  
<https://doi.org/10.1016/j.procir.2017.12.204>

### **Publisher's note**

Whioce Publishing remains neutral with regard to jurisdictional claims in published maps and institutional affiliations.